JCI insight

RESEARCH ARTICLE

Nrf2/antioxidant pathway mediates β cell self-repair after damage by high-fat diet–induced oxidative stress

Tsehay Abebe,[1] Jana Mahadevan,[1,2,3,4] Lindsey Bogachus,[1,2,3,5] Stephanie Hahn,[1] Michele Black,[6] Elizabeth Oseid,[1] Fumihiko Urano,[4] Vincenzo Cirulli,[2,3] and R. Paul Robertson[1,2,3,5]

[1]Pacific Northwest Diabetes Research Institute, Seattle, Washington, USA. [2]Division of Metabolism, Endocrinology, and Nutrition, Department of Medicine, and [3]Department of Pharmacology, University of Washington, Seattle, Washington, USA. [4]Department of Endocrinology, Metabolism, and Lipid Research, Washington University School of Medicine, St. Louis, Missouri, USA. [5]Division of Endocrinology and Metabolism, Department of Medicine, University of Minnesota, Minneapolis, Minnesota, USA. [6]Department of Immunology, University of Washington, Seattle, Washington, USA.

Many theories have been advanced to better understand why β cell function and structure relentlessly deteriorate during the course of type 2 diabetes (T2D). These theories include inflammation, apoptosis, replication, neogenesis, autophagy, differentiation, dedifferentiation, and decreased levels of insulin gene regulatory proteins. However, none of these have considered the possibility that endogenous self-repair of existing β cells may be an important factor. To examine this hypothesis, we conducted studies with female Zucker diabetic fatty rats fed a high-fat diet (HFD) for 1, 2, 4, 7, 9, 18, or 28 days, followed by a return to regular chow for 2–3 weeks. Repair was defined as reversal of elevated blood glucose and of inappropriately low blood insulin levels caused by a HFD, as well as reversal of structural damage visualized by imaging studies. We observed evidence of functional β cell damage after a 9-day exposure to a HFD and then repair after 2–3 weeks of being returned to normal chow (blood glucose [BG] = 348 ± 30 vs. 126 ± 3; mg/dl; days 9 vs. 23 day, $P < 0.01$). After 18- and 28-day exposure to a HFD, damage was more severe and repair was less evident. Insulin levels progressively diminished with 9-day exposure to a HFD; after returning to a regular diet, insulin levels rebounded toward, but did not reach, normal values. Increase in β cell mass was 4-fold after 9 days and 3-fold after 18 days, and there was no increase after 28 days of a HFD. Increases in β cell mass during a HFD were not different when comparing values before and after a return to regular diet within the 9-, 18-, or 28-day studies. No changes were observed in apoptosis or β cell replication. Formation of intracellular markers of oxidative stress, intranuclear translocation of Nrf2, and formation of intracellular antioxidant proteins indicated the participation of HFD/oxidative stress induction of the Nrf2/antioxidant pathway. Flow cytometry–based assessment of β cell volume, morphology, and insulin-specific immunoreactivity, as well as ultrastructural analysis by transmission electron microscopy, revealed that short-term exposure to a HFD produced significant changes in β cell morphology and function that are reversible after returning to regular chow. These results suggest that a possible mechanism mediating the ability of β cells to self-repair after a short-term exposure to a HFD is the activation of the Nrf2/antioxidant pathway.

Authorship note: T. Abebe and J. Mahadevan contributed equally to this work.

Conflict of interest: The authors have declared that no conflict of interest exists.

Submitted: January 31, 2017
Accepted: November 15, 2017
Published: December 21, 2017

Reference information:
JCI Insight. 2017;2(24):e92854.
https://doi.org/10.1172/jci.insight.92854.

Introduction

Many phenomena have been extensively investigated to examine their potential roles in the relentless decline of β cell mass and function that is characteristic of type 2 diabetes (T2D) in humans (1–21). In virtually all these lines of study, the β cell itself has been tacitly assumed to play the passive role of victim during its exposure to hyperglycemia. In some reports, oxidative stress caused by hyperglycemia has been suggested to be an operative mechanism in the continuation of β cell decline after the initiating (probably genetic) mechanism is triggered (22–26). We are unaware of any previous studies that directly address the hypothesis that, early in T2D, β cells spontaneously initiate an effort to repair themselves. Our rationale for examining this hypothesis stems from our previous work with db/db mice, a rodent model of T2D, in

which the β cells specifically overexpressed an insulin-promoter–driven glutathione peroxidase (GPx) transgene (27). WT db/db animals fed a high-fat diet (HFD) developed severe hyperglycemia. The GPx-transgenic mice also initially become hyperglycemic early after starting a HFD but, soon thereafter, reversed this trend and, within weeks, normalized their blood glucose levels. The rapidity with which the glucose levels reverted to normal in the transgenic mice could not be explained by changes in rates of apoptosis or in rates of β cell replication. Therefore, we considered the possibility that we had serendipitously witnessed an active process of self-repair of existing β cells via intrinsic GPx production that decreased oxidative stress and thereby facilitated a return of normal β cell function and structure.

With this background information, we designed the studies described herein to examine the hypothesis that, during acute hyperglycemia, β cells undergo oxidative stress (28–31) and, in response, spontaneously initiate endogenous repair mechanisms. We hypothesized that 1 mechanism might be the KEAP-1/nuclear factor erythroid-derived-2-related-factor (Nrf2)/antioxidant pathway, widely recognized as a prominent regulator of antioxidant enzyme gene expression (32–36). Several reports involving mouse models of diabetes appeared midway through our study and supported this possibility (6, 37–39). Our current work used Zucker diabetic fatty rats (ZDF rats) that are known to develop severe hyperglycemia and oxidative stress when fed a HFD (40). The design involved an initial baseline period of a regular chow (17% fat) diet followed by exposure to a HFD (48% fat) for increasing lengths of time, and then an intervention period during which the HFD was removed and the regular chow diet was resumed. No other manipulations involving drugs or diets were used. For the purposes of this study, we defined β cell repair as reversal of functional damage by measuring blood glucose and insulin levels and reversal of structural damage by fluorescent imaging of insulin, markers of oxidative stress (4HNE and 8-OHdG), and Nrf2, HO-1, SOD-1, and SOD-2. In addition, we used a flow cytometry–based method (ImageStream) to assess β cell volume, morphology and insulin-specific immunoreactivity, and transmission electron microscopy (TEM) to determine if short-term exposure to a HFD produces significant alterations in β cells that are reversible after returning to regular chow. We sought answers to the following questions: (i) are acute hyperglycemia and relatively low insulin levels in ZDF rats during a brief exposure to a HFD related to oxidative stress and β cell structural damage, and do these appreciably worsen with longer exposure to a HFD; (ii) does duration of antecedent exposure to a HFD influence the degree to which β cells repair themselves when they are returned to low-fat diets; and (iii) is there evidence that the mechanism by which β cells initiate self-repair is activation of the KEAP-1/Nrf2 pathway with consequent formation of intracellular antioxidant proteins?

Results

Metabolic studies. During the 3-week baseline period of this study in which a standard 17% fat regular chow diet was used, nonfasting blood glucose levels were in the normal range (115 ± 3 mg/dl, n = 76). When 68 animals were switched to a 48% HFD, they promptly developed hyperglycemia (Supplemental Table 1; supplemental material available online with this article; https://doi.org/10.1172/jci.insight.97381DS1). Glucose levels in the group (n = 8) that continued the 17% fat diet remained normal.

The 1- to 9-day HFD withdrawal study: group A. HFD was withdrawn from 5 subgroups of 4 rats each that developed various levels of hyperglycemia over 1, 2, 4, 7, and 9 days in direct relationship to the length of time they consumed a HFD (Figure 1A and Supplemental Table 1). After withdrawing the HFD and returning to standard 17% fat diet, the blood glucose levels for all 5 groups returned to the normal range. However, the rate of return to normoglycemia for the rats that consumed a HFD for 9 days appeared to be slower than that of the other rat subgroups, and their plasma insulin levels began to fall while eating a HFD (data not shown). We interpreted the slower rate of glycemia normalization and the decreased insulin levels after 9 days of a HFD as a first evidence that β cell function was failing. Hence, we chose to further investigate the 9-day HFD reversal group with additional methods that included a quantitative flow cytometry–based approach (ImageStream) to assess insulin expression and volume, and by ultrastructural analysis of β cell morphology (TEM) to identify possible changes in β cell organelle integrity. To further develop these studies, we also extended our metabolic analysis to additional groups of rats that were exposed to a HFD for longer periods of time.

The 9-day HFD withdrawal study: group B. After withdrawing HFD on day 9 from a new subgroup of 4 hyperglycemic rats and resuming the standard 17% fat diet, we observed that, by day 15 of reversing the diets, blood nonfasting glucose levels returned to the normal range (126 ± 3 mg/dl; $P < 0.01$; Figure 1B and Supplemental Table 1). Blood glucose levels remained normal for 7 more days, and then pancreata were

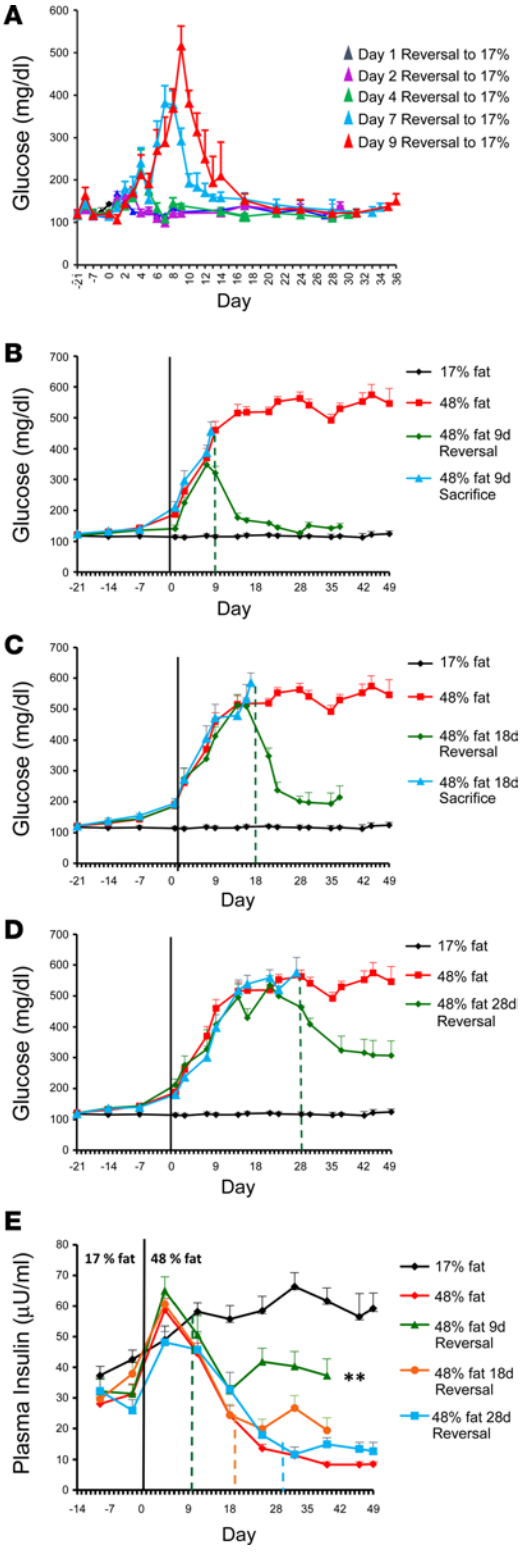

Figure 1. Induction of hyperglycemia by a high-fat (48%) diet followed by spontaneous return to toward normoglycemia after switching to regular (17% fat) diets. (**A–D**) The durations of exposure to high-fat diets were 1, 2, 4, 7, 9, 18, and 28 days prior to a return to regular diets. The degrees of hyperglycemia were progressively worse and the returns toward normoglycemia were progressively slower as the length of exposure to high-fat diets was increased. All glucose levels were obtained under nonfasting conditions. (**E**) Insulin levels at the end of the studies were lowest in the ZDF rats fed 45% fat diet exclusively and highest in the animals fed 17% fat diets exclusively. Insulin levels in the 3 groups of animals fed high-fat diets for variable time periods followed by a return to regular diets had intermediate plasma insulin levels. The highest insulin levels during the return to regular diets were in animals with the shortest exposure (9 days) to the high-fat diets, while longer exposures to high-fat diet (18 and 28 days) were associated with increasingly lower insulin levels after return to low-fat diets. However, even in the 9-day reversal study, insulin levels failed to reach the levels observed in the control animals fed 17% fat standard chow diets. Two-tailed Student *t* tests with Bonferroni correction for multiple comparison testing; $^{**}P < 0.01$.

removed for imaging studies. Another subgroup of 4 hyperglycemic rats underwent pancreatic resection on day 9 for imaging studies, while still being fed the 48% fat diet. The 2 dietary control groups of 8 animals each (continuous HFD or standard diets) were fed a HFD or standard diet without change until the day 46, when their pancreata were removed for imaging studies.

The 18-day HFD withdrawal study: group C. On day 18, the 48% fat diet was withdrawn from a subgroup of 4 hyperglycemic rats and the 17% fat diet was resumed. By day 29, their blood glucose levels had declined (Figure 1C and Supplemental Table 1) to and plateaued at 215 ± 37 mg/dl, significantly higher those observed at the conclusion of the 9-day study described above (126 ± 3 mg/dl, $P < 0.001$). Another subgroup of 4 hyperglycemic rats underwent pancreatic resection on day 18 for imaging studies, while still being fed the 48% fat diet. The 2 dietary control groups of 8 animals each (continuous HFD or standard diets) were fed a HFD or standard diet without change until day 46, when their pancreata were removed for imaging studies.

The 28-day HFD withdrawal study: group D. On day 28, the 48% fat diet was withdrawn from a subgroup of 4 hyperglycemic rats, and the 17% fat diet was resumed. By day 42, their blood glucose levels had declined (Figure 1D and Supplemental Table 1) and plateaued at 307 ± 47 mg/dl, significantly higher than those observed at the conclusion of the 9-day study described above (126 ± 3 mg/dl, $P < 0.001$). Another subgroup of 4 hyperglycemic rats underwent pancreatic resection on day 28 for imaging studies, while still being fed the 48% fat diet. The 2 dietary control groups of 8 animals each (continuous HFD or standard diets) were fed a HFD or standard diet without change until day 46, when their pancreata were removed for imaging studies.

Body weights, plasma insulin, i.p. glucose tolerance test (IPGTT), insulin tolerance test (ITT), and β cell mass. No differences in body weights were observed among the 7 groups of animals at any one of the experimental time points (1, 2, 4, 7, 9, 18, or 28 days). Compared with baseline values, plasma insulin values initially rose on regular diet but thereafter were lower in Groups B, C, and D on a HFD (Figure 1E). In none of these groups, after reversal to regular diet, did insulin levels reach the height of the levels attained by the control animals fed a regular chow diet only. Measures of glucose tolerance during IPGTT in the HFD deteriorated by day 9 and remained abnormal, despite reversal to regular diets through day 30 (Figure 2A). Insulin levels at the end of the IPGTT were not different, although the reversed HFD group had a delay in developing insulin increments (Figure 2B). Measures of insulin sensitivity during ITT in the 3 subgroups revealed no significant differences (Figure 2C). The β cell mass in the ZDF rats fed a HFD for 9 days was 4-fold greater than Zucker lean control rats (ZLC rats; 8.5 ± 1.5 mg vs. 2.9 ± 0.9 mg, $P < 0.001$; Figure 3A). There was a progressive decrease in β cell mass after 18 and 28 days of a HFD, compared with the 9-day values. However, there were no significant differences in β cell mass values within any of the 3

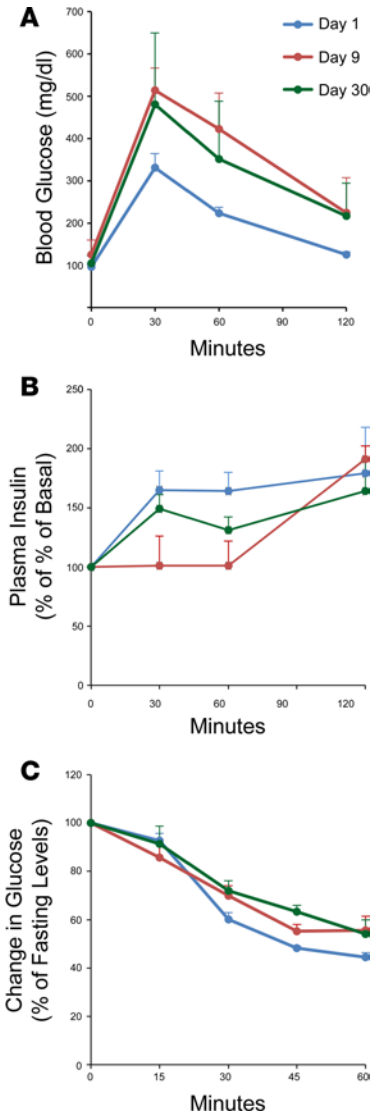

Figure 2. Glucose tolerance and insulin tolerance test results. Blue line indicates controls on regular chow; green line indicates high-fat diet (HFD) for 9 days; orange line indicates HFD for 9 days and then reversal to regular chow for 21 more days. (**A** and **B**) Glucose tolerance test (i.p., 120 minutes). (**A**) Glucose tolerance (i.p.) in both 9-day HFD groups (green and orange lines) deteriorated despite reversal of 1 HFD group to regular chow on day 9 through day 30. (**B**) Insulin levels during IPGTT were not different, although the HFD group that was reversed from HFD had a delay in developing insulin increments. (**C**) Insulin tolerance test (60 minutes). Glucose fell to similar levels during ITT on baseline regular diet and on a HFD, despite reversal of 1 HFD group to regular chow on day 9 through day 30. Consequently, no differences in insulin sensitivity were observed.

dietary subgroups (9-, 18-, or 28-day HFD with or without diet reversal). Morphometric assessment of insulin-specific immunoreactivity revealed a significant reduction of insulin granulation, which was reversible upon returning the animals to a regular diet (Figure 3B).

Reduced insulin expression in β cells exposed to a HFD. Based on the observed functional alteration of β cell performance in animals fed a HFD (Figure 1 and Figure 2), and based on our immunolocalization studies pointing to reduced insulin expression (Figure 3), we conducted experiments in which we took advantage of a technology called ImageStream, which merges flow cytometry with multichannel brightfield, darkfield, and fluorescent imaging of individual cells under flow conditions (41, 42). Pancreatic islets from either ZDF controls, ZDF rats fed with a HFD for 9 days, and ZDF animals reversed to regular chow were dissociated into a single cell suspension and processed for intracellular staining for insulin and DNA (DAPI). Cells were then analyzed using an Amnis ImageStream X Mark II imaging cytometer. After data acquisition, cells imaged as "in focus" exhibited heterogeneous size distribution, with a slight decrease in values of the brightfield area (Figure 4, A, D, and G). Contrary to cell area measured in conventional optical microscopy, "brightfield area" provides a more accurate estimation of cell size (or volume). In agreement with previous observations showing that β cell size can decrease during the first 3 months of exposure to a HFD, and later followed by β cell hyperthrophy after 6 and 12 months of HFD feeding (43), our ImageStream analysis suggests that even a short-term exposure to a HFD may have a significant impact on the overall homeostasis of β cell volume. Interestingly, results from this analysis also revealed that the geometric mean intensity of insulin-specific immunoreactivity detected in cells gated from the "in focus" population was decreased by ~45% (from 305,362 to 173,261 ImageStream X Mark II arbitrary units) in β cells from ZDF-HFD (Figure 4, B and E). This decrease in insulin immunoreactivity appeared fully recovered and surpassed levels detected in control ZDF islets (up to 686,692 ImageStream X Mark II arbitrary units; Figure 4H). Representative examples of imaged β cells from control ZDF (Figure 4C), HFD (Figure 4F), and reversed animals (Figure 4I) provide a qualitative assessment of this analysis.

Islet morphology, markers of oxidative stress, proliferation, and apoptosis. Morphological evidence for β cell damage could be observed as early as day 9 under the HFD condition, with islets appearing ragged in shape and with substantially reduced insulin granulation (Figure 5, A and B). After reversal to the regular diet in the 9-day study, islets completely recovered normal morphology and regained near-normal staining for insulin (Figure 5C). There was less improvement in β cell morphology during a return to regular diet after 18 days of the HFD and very little improvement after a return to regular diet after 28 days of the HFD (not shown). Morphometric analysis for markers of oxidative stress revealed that β cells from rats fed a HFD for 9 days showed intense cytoplasmic staining for 4HNE (Figure 5B) (and for 8-OH-dG, data not shown). After the animals were returned to a regular diet, the immunoreactivity for 4HNE was significantly reduced (Figure 5, C and D). Nuclear staining for Nrf2 was also prominent in rats fed HFDs for 9 days (Figure 5F), compared with ZDF controls (Figure 5E), with an expression pattern that appeared both nuclear and cytoplasmic. Immunoreactivity for Nrf2 was also reduced after returning to a regular diet (Figure 5, G, and H). Nuclear and perinuclear staining for HO-1 was also observed in animals exposed to a HFD for 9 days (Figure 5J), compared with ZDF controls (Figure 5I); after a return to a regular diet, very little HO-1 staining was observed (Figure 5, K and L). Rats fed a 48% fat diet for 9, 18, and 28 days and sacrificed — as well as those returned to a regular diet for 2 weeks — did not stain for Ki-67 (data not shown). Apoptotic positive cells were evident in the ZDF rats treated with a HFD, whereas no apparent differences in apoptotic cells were noticed after a return to the regular diet for 9, 18, and 28 days (data not shown). However, the low frequency of TUNEL-positive cells precluded meaningful quantification.

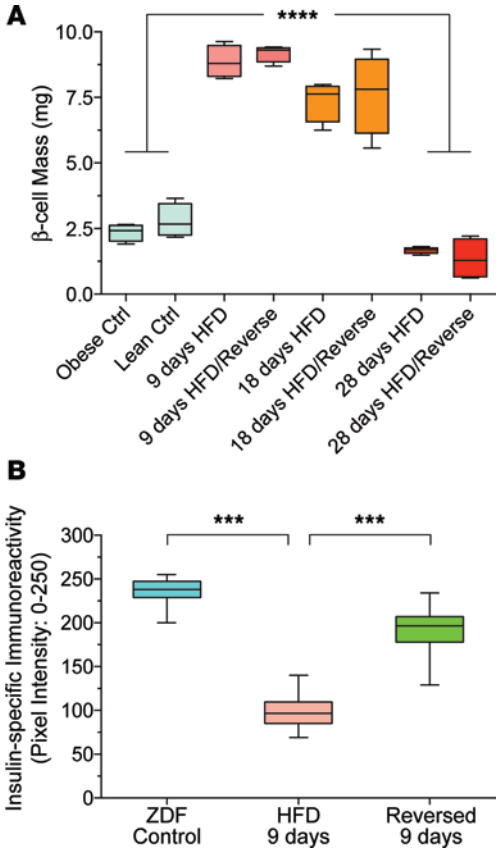

Figure 3. β Cell mass. (**A**) The group receiving HFD for 9 days developed a significantly greater β cell mass compared with controls fed 17% fat standard chow. However, with longer exposure to the HFD, there were progressively smaller increases in β cell mass after 18- and 28-day HFD. Return to regular diets did not alter β cell mass in any of the 3 groups whose HFDs were reversed to regular chow diets. Reverse indicates reversal to regular diet after 9, 18, or 28 days of high-fat diet. (**B**) Quantitative determination of pixel intensity for insulin-specific immunofluorescent signal measured in pancreatic sections from ZDF controls, HFD 9 days, and Reversed 9 days animals. Morphometric measurements were performed on 57, 64, and 73 sections per animal group, respectively. Two-way ANOVA, ***$P < 0.005$; ****$P < 0.0001$.

As separate assessments of the KEAP-1/Nrf2/antioxidant pathway, we examined islets from hyperglycemic male ZDF rats and hyperglycemic male db/db mice in which we have previously shown to have increased cytoplasmic levels of 8-OH-dG and 4HNE (27, 40). These experiments revealed that the hyperglycemic male ZDF rats that were fed a HFD demonstrated substantial staining for Nrf2 (Figure 6A), both cytosolic and nuclear, whereas simultaneously feeding these animals the antioxidant Ebselen, while on a HFD, prevented the appearance of Nrf2-specific immunoreactivity (Figure 6B). Similarly, WT hyperglycemic diabetic db/db mice that had been fed a HFD demonstrated intranuclear staining of Nrf2 (Figure 6C), but this was not the case for normoglycemic db/db mice, in which we had β cell–specifically expressed the transgene for the antioxidant GPx-1 (db/db-GPx-$1^{+/+}$ male mice; Figure 6D).

Collectively, these data from ZDF and db/db animals (Figure 6) add significant validation to our hypothesis and support the concept that oxidative stress associated with a HFD may result in β cell damage in multiple models of T2D. Importantly, the results also underline the effectiveness of antioxidant interventions in preventing and/or reversing HFD-induced β cell damage.

Altered β cell morphology caused by short-term HFD can be reversed. In a separate set of experiments, we investigated the morphology of β cells at the ultrastructural level by TEM. For these studies, we focused on 3 groups of animals: control ZDF rats fed with regular chow, ZDF animals fed with a HFD for 9 days, and a group fed a HFD for 9 days and then switched to regular chow for an additional 21 days. As can be observed in Figure 7, A–C, β cells from ZDF control animals revealed a normal ultrastructural appearance, with an abundant content of insulin secretory granules exhibiting classical electron-dense crystallized insulin cores, and a normal rough ER (RER) populated by electron-dense spots, compatible with ribosomal content (Figure 7C, arrowheads). In contrast, animals fed with a HFD (Figure 7, D–H) exhibited marked alterations with dysmorphic secretory vesicles, some of them with little crystalline insulin (Figure 7D, arrowheads), disorganized Golgi apparatus (Figure 7E, asterisks), numerous autophagic bodies (Figure 7F, black arrowheads), and increased cytosolic-free ribosomes not associated with the ER (Figure 7F, white arrowheads) that presented enlarged cisternae with reduced ribosomal content (Figure 7H, arrowheads). Interestingly, animals that were reversed to a regular chow diet for 21 days after the initial period of 9 days on a HFD revealed a normalization of most of these abnormalities (Figure 7, I–K), with β cells exhibiting an increased frequency of insulin-containing secretory vesicles whose morphology appeared indistinguishable from that observed in the control animal group. In addition, autophagic bodies were almost undetectable, and the RER regained a well-organized multilayered arrangement (Figure 7, I–K, arrowheads). These results provide direct morphological validation at the ultrastructural level for the deleterious effects of a HFD on β cells and their reversibility following a return to regular chow. Collectively, our results uncover an important window of opportunity for therapeutic interventions within the first 9 days of exposure to a HFD, which could prevent progressive β cell dysfunction, averting diabetes.

Discussion

This study examined the potentially novel hypothesis that rodents fed a HFD, and thereby exposed to acute hyperglycemia and oxidative stress, activate the KEAP-1/Nrf2/antioxidant pathway as a mechanism to initiate endogenous β cell self-repair. ZDF rats fed a HFD for 1–28 days became hyperglycemic with initially high but eventually low insulin levels and abnormal β cell structure. Returning to a 17% fat standard chow diet improved β cell function so that elevated glucose levels fell and low insulin levels increased. The completeness

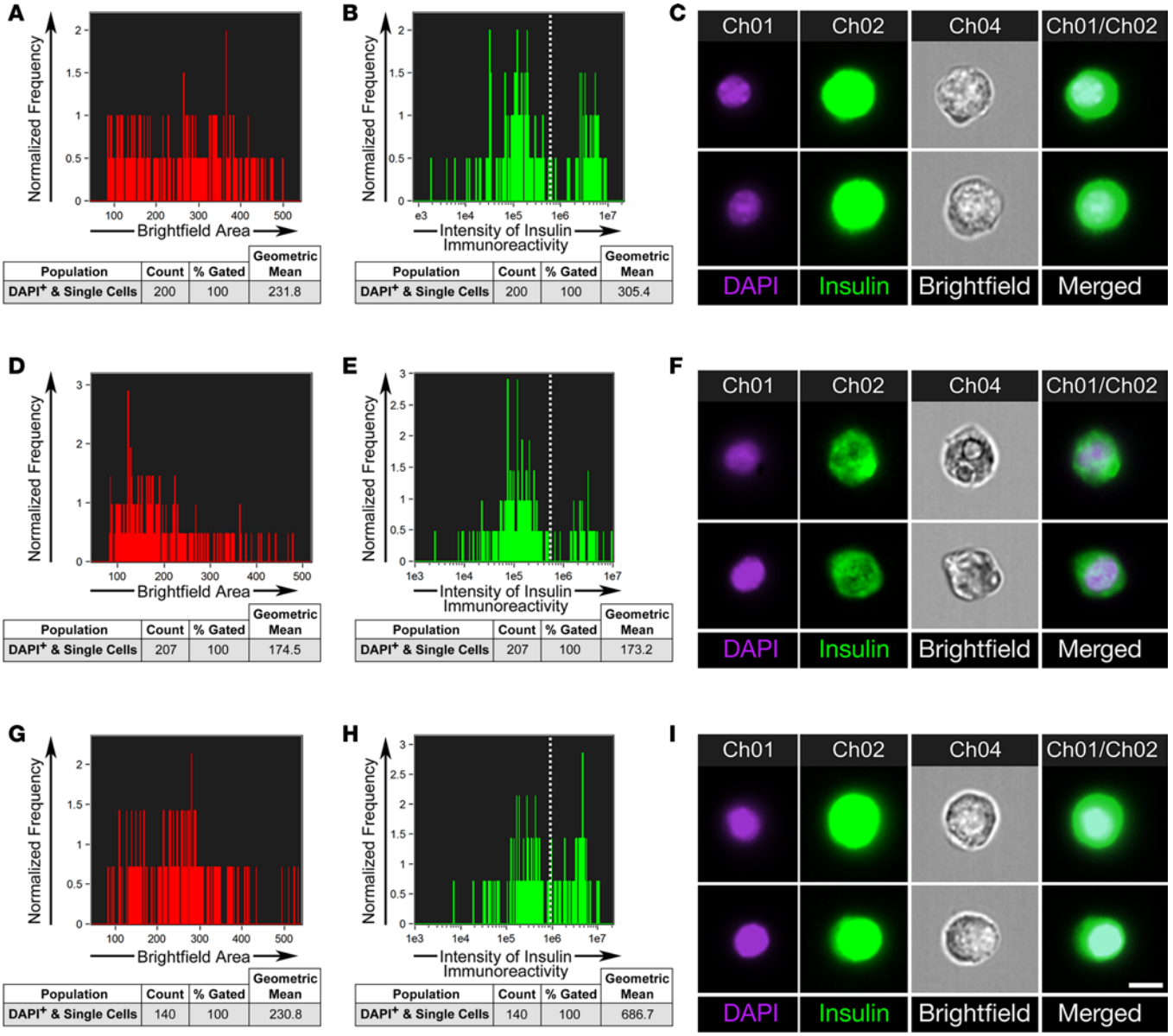

Population	Count	% Gated	Geometric Mean
DAPI+ & Single Cells	200	100	231.8

Population	Count	% Gated	Geometric Mean
DAPI+ & Single Cells	200	100	305.4

Population	Count	% Gated	Geometric Mean
DAPI+ & Single Cells	207	100	174.5

Population	Count	% Gated	Geometric Mean
DAPI+ & Single Cells	207	100	173.2

Population	Count	% Gated	Geometric Mean
DAPI+ & Single Cells	140	100	230.8

Population	Count	% Gated	Geometric Mean
DAPI+ & Single Cells	140	100	686.7

Figure 4. ImageStream flowcytometric analysis of β cells. Islet cells from control ZDF (**A–C**), HFD (**D–F**), and reversed ZDF animals (**G–I**), analyzed for their brightfield area versus DNA (DAPI) content (**A**, **D**, and **G**), insulin-specific immunoreactivity (**B**, **E**, and **H**), morphological appearance (**C**, **F**, and **I**). Notable differences include slight reduction in β cell size (**D**) and a reduced insulin-specific immunoreactivity in HFD animals (**E**). These alterations were not observed in the diet-reversed animal group (**G** and **H**). Representative of $n = 2$ separate determinations, with islets isolated from 2 animals per experimental group. Scale bar: 7 μm.

with which the animals reestablished normal glucose and insulin levels was inversely related to the length of time they had been exposed to a HFD. Although glucose levels during IPPGT were significantly higher during a HFD than baseline values on a regular diet, there were not significant improvements in glucose levels after a return to a regular diet. In addition, there were no significant differences in final insulin values after IPGTT, nor in glucose levels during ITT. That these values from functional testing were not dramatically different despite the impressive differences in β cell structure strongly supports the conclusion that initial structural changes led to changes in function, rather than vice-versa. No differences were observed in β cell mass values within specific experimental groups, but returning to standard chow early in the course reversed abnormalities in β cell structure. All these changes occurred in the absence of changes in β cell apoptosis or proliferation.

Intriguingly, our analysis of individual β cells by ImageStream flowcytometry — while quantitatively validating a reduced insulin-specific immunoreactivity in HFD animals — also revealed a slight reduction in β cell size. This paradoxical observation agrees with previous work showing that, although long-term

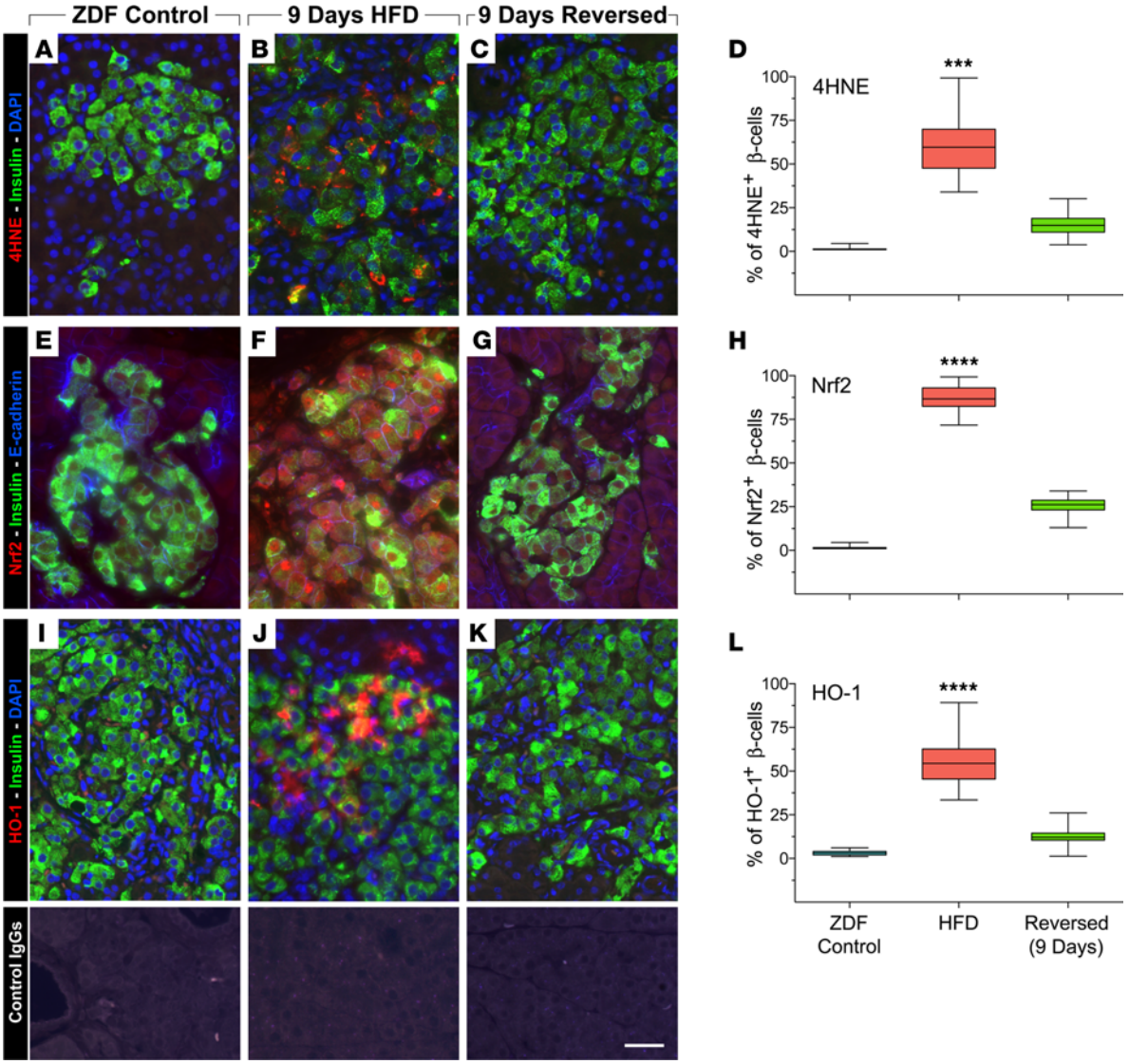

Figure 5. Markers of oxidative stress. (**A**) Pancreatic sections were double labeled for insulin (green fluorescence) and 4-HNE (red fluorescence). ZDF rats after 9 days of high-fat diet showed intense cytoplasmic staining for 4-HNE in β cells (**B**). This was reduced 2 weeks after a return to regular diets (**C**). Percentage of 4-HNE$^+$ β cells in each animal group (**D**). Immunostaining for Nrf2 (red fluorescence) revealed substantial immunoreactivity both in the cytoplasm and the nucleus of β cells in ZDF rats fed high fat diets for 9 days (**F**), when compared with ZDF controls (**E**). In contrast, 2 weeks after return to regular diets, the immunoreactivity for Nrf2 was dramatically reduced (**G**). Percentage of 4-Nrf2$^+$ β cells in each animal group (**H**). Similarly, pancreatic sections stained for HO-1 (red fluorescence) showed increased cytoplasmic and nuclear localization of HO-1 in β cells (green fluorescence), which – after 9 days of HFD – was greatly diminished 2 weeks after return to regular diet (**K**). Percentage of HO-1$^+$ β cells in each animal group (**L**). Specificity of detected immunoreactivities was validated by incubation of tissue sections with control IgGs from each species (lower panels). Scale bar: 25 μm. (**D**, **H**, and **L**) One-way ANOVA, ***$P < 0.005$, ****$P < 0.0001$.

HFD leads to an increase in β cell volume, there is a significant heterogeneity and reduction in β cell size during the first 3 months (43). These events were accompanied by the appearance of intracellular markers of oxidative stress; translocation of cytoplasmic Nrf2 to the nucleus; activation of antioxidant genes as evidenced by formation of the intracellular antioxidant proteins; improved β cell structure with insulin regranulation; and eventually diminution of markers of oxidative stress.

We have suggested that oxidative stress is a central mechanism for in vitro and in vivo glucose toxicity of β cells (28, 29). Our previous studies of islets (30–31) and those of others (21) reported preventive effects of exogenous antioxidants on the development of adverse effects on β cell mass and function caused by prolonged exposure to high glucose concentrations. Our current observations are in keeping with those recently reported (6, 37–39). Butler and colleagues reported that islets from autophagy-deficient mice had increased oxidative damage in β cells associated with a failed response of Nrf2 to oxidative stress (6).

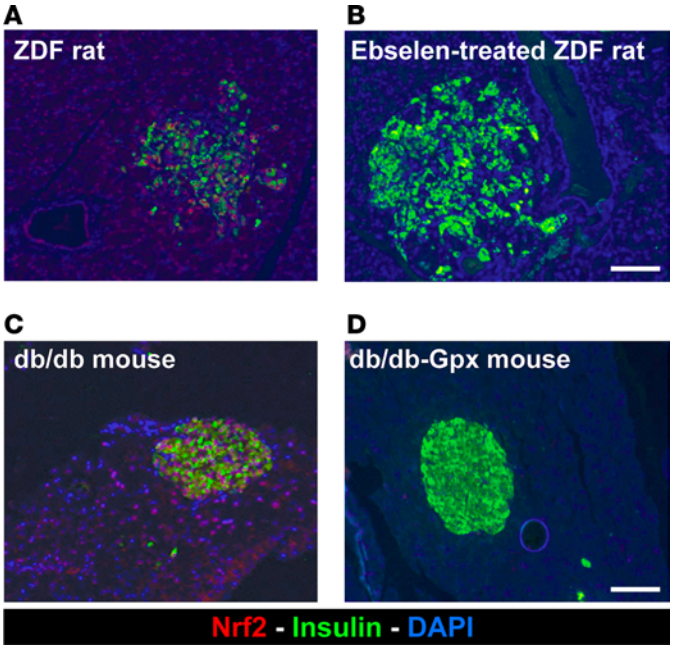

Figure 6. Nrf2 staining in 2 additional diabetic animal models. Pancreatic sections from hyperglycemic male ZDF rats showed substantial immunostaining for Nrf2 (**A**, red fluorescence), in β cells (green fluorescence), whereas ZDF rats fed with the antioxidant Ebselen along with the high-fat diet for 6 weeks did not stain for Nrf2 (**B**). (**C**) Hyperglycemic WT db/db mice fed a high-fat diet showed increased immunoreactivity for Nrf2 in β cells, whereas db/db mice with β cell–specific overexpression of GPx-1 fed a high-fat diet showed no detectable staining for Nrf2 (**D**). Scale bars: 50 μm.

Yagishita et al. (37) studied the KEAP-1/Nrf2 pathway in the context of exogenous cytokine inducers of oxidative stress. They used 4 genetically modified mouse models: β cell–specific KEAP-1 KO, β cell–specific Nrf2 heterozygous KO, conventional Nrf2 KO, and β cell–specific Nrf2 conditional KO. They concluded that Nrf2 induction by oxidative stress counteracts cytokine-induced oxidative damage in β cells and, therefore, that the KEAP-1/Nrf2 system is an important defense pathway for protecting β cells. Uruno et al. (38) reported that genetic activation of Nrf2 in KEAP-1–KO mice suppressed the onset of diabetes in db/db mice and that induction of Nrf2 activity by an oral imidazole derivative markedly improved insulin secretion during oral glucose tolerance test (OGTT). Masuda et al. (39) studied the effects of a different Nrf2 activator (dh404) on human islets obtained from cadaveric donors and reported that this agent increased intranuclear Nrf2 levels and increased mRNA levels for several different antioxidant proteins.

Our current observations agree with these authors regarding the potential importance of the KEAP-1/Nrf2/antioxidant pathway in defending β cells against the adverse effects of oxidative stress. Essential differences between the previous studies and the ones we now report are that we used the more physiologic and clinically relevant paradigm of a HFD feeding over increasing periods of time rather than subjecting β cells to cytokines, islet amyloid polypeptide (IAPP), or trauma (cadaveric islet isolation) to examine intrinsic β cell responses to stress. We also report the associated increased levels of markers of oxidative stress (8-OHdG and 4HNE) in β cells, caused by a HFD, as well as the increased β cell levels of downstream targets of Nrf2 activation. Moreover, we present data from 2 other models of glucose toxicity in HFD-fed animals. One is the male ZDF rat treated with placebo or the oral antioxidant Ebselen (40). The other is the female db/db transgenic mouse that overexpresses GPx specifically in β cells (27). In both models, we show that the control animals (hyperglycemic with markers of oxidative stress; refs. 27, 40) exhibit pronounced Nrf2 immunoreactivity, whereas animals treated with Ebselen or mice overexpressing GPx in β cells do not. Finally, our analysis by electron microscopy demonstrates that grossly altered ultrastructural features in β cells after a HFD feeding can be corrected by a return to regular chow, further substantiating the reversibility of structural abnormalities caused by a short period on a HFD.

Most importantly, the current work uniquely demonstrates that existing rodent β cells can initiate self-repair in response to oxidative stress in very early but not later stages of oxidative damage caused by a HFD and hyperglycemia. An alternative possibility is that, since ZDF rats also become hypertriglyceridemic, excess circulating lipid rather than glucose may be the inciting factor for β cell damage. However, this does not seem likely to be the case because prevention of hyperglycemia by phlorizin treatment normalizes glycemia and prevents the development of defects in insulin gene expression in ZDF rats fed a HFD, whereas prevention of hypertriglyceridemia by bezafibrate in the same model does not (24).

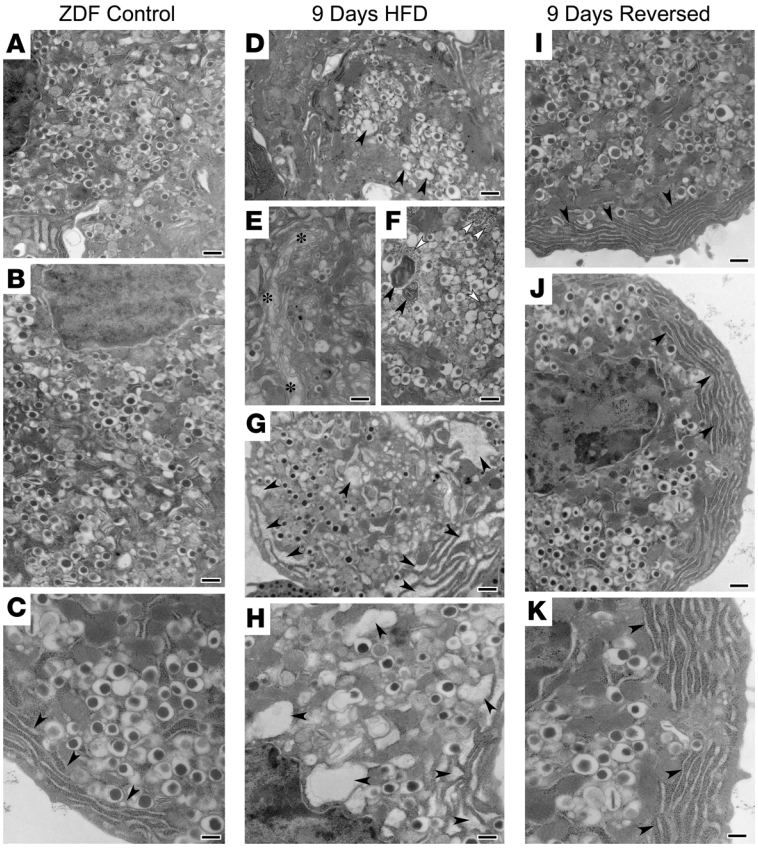

Figure 7. Ultrastructural analysis of β cells by transmission electron microscopy (TEM). Examples of β cells from control ZDF (**A–C**), HFD (**D–H**), and diet-reversed ZDF animals (**I–K**). β Cells in control ZDF rats exhibit normal-looking distribution of secretory granules with the classical electron-dense crystallized insulin cores and normal rough endoplasmic reticulum (RER) (**C**, arrowheads). Marked alterations can be noted in β cells from animals fed with HFD, including dysmorphic secretory vesicles (**D**, arrowheads), disorganized Golgi apparatus (**E**, asterisks), numerous autophagic bodies (**F**, black arrowheads), increased cytosolic free ribosomes (**F**, white arrowheads), and substantial enlarged ER cisternae (**G** and **H**, arrowheads). These alterations were not found in β cells from diet-reversed animals, which exhibited normalized insulin granule distribution and well-organized ER (**I–K**, arrowheads). TEM analysis was performed on islets isolated from each experimental group (n = 2 animals per group). Images acquired from at least n = 20 nonconsecutive ultrathin sections per experimental group. Representative of n = 3 separate determinations. Scale bars: 300 nm (**A**, **B**, **D–G**, **I**, and **J**) and 70 nm (**C**, **H**, **K**).

In conclusion, our studies demonstrate that hyperglycemia caused by a HFD causes oxidative stress and acute β cell injury in female ZDF rats. A return to a regular diet within 9 days resolved hyperglycemia and diminished oxidative stress, and it allowed endogenous β cell repair that could not be related to changes in apoptosis, replication, or increases in β cell mass. The findings of Nrf2-specific immunoreactivity, both cytosolic and nuclear, as well as formation of increased endogenous antioxidant protein in repaired β cells, provide potentially novel evidence that suggests the KEAP-1/Nrf2/antioxidant pathway plays a role in β cell self-repair. The translational relevance of these observations lies in our evidence that prompt reversal of acute hyperglycemia allows β cells to repair themselves. These results also indicate that this acute phase of β cell repair identifies a point of no return, beyond which the degree of repair is insufficient to return β cells to full function. This clearly pertains to management of clinical hyperglycemia in humans and suggests that prompt management to resolve states of even mild degrees of impaired glucose tolerance may facilitate maintenance of β cell integrity and function, and potentially prevent progression to T2D.

Methods

Laboratory animals. Six-week-old female WT (+/+) obese ZDF rats and (+/–) lean ZDF rats were purchased from Charles River Labs. Females rather than males were chosen because they have a less severe form of diabetes compared with male animals and therefore seemed more likely to undergo self-repair of β cells. Upon arrival, they acclimated for 3 weeks and were ad lib fed a 17% fat diet (Formulab Diet 5008, Animal Specialties). Animals were weighed and nonfasting blood glucose measurements were obtained weekly using an Alphatrak hand-held glucose meter (Abbott Laboratories). On day 0, animals either continued the 17% fat diet or were switched to a 48% fat diet (RD12468, Research Diets). Weight, blood glucose, and plasma insulin levels were measured for the duration of the study. Eight groups of 8 animals were fed the 48% fat diet for 1, 2, 4, 7, 9, 18, or 28 days; at each of these time points, 4 subgroups of animals in each group were sacrificed, and the 4 others were switched back to the 17% fat diet. The latter animals were maintained on a 17% fat diet for an additional 2–3 weeks and then were sacrificed. Two additional control groups of 8 animals each were fed either 17% or 48% fat diets from day 0 until the end of the study, with no dietary interventions. At sacrifice, pancreata were harvested, fixed in 10% neutral buffered formalin, processed, and embedded in paraffin for sectioning.

Measurements of nonfasting glucose and insulin levels. Glucose was measured via tail vein puncture, using a handheld meter designed for measuring rodent blood glucose (Alphatrak meter, Abbot Laboratories). Larger quantities of tail vein blood were drawn to obtain serum that was frozen at –20°C and later used to measure insulin using a Rat/Mouse Insulin EIA from MilliporeSigma. Insulin tolerance testing was performed to assess insulin sensitivity, and i.p. glucose tolerance testing was performed to assess β cell function, both as previously described (40).

Immunostains for insulin and measurements of β cell mass, proliferation, and apoptosis. Pancreata were removed from ZDF rats and fixed overnight with 4% formalin. Fixed tissues were processed for paraffin embedding, and 4 μm sections were prepared and mounted on slides. Each slide was treated with H_2O_2 solution to inactivate endogenous peroxidase. Heat-induced antigen retrieval was carried out using antigen unmasking solution (Vector Laboratories). The sections were washed twice with Tris-buffered saline (pH 7.4) containing 0.1% Tween-20 (TBST). Normal donkey serum (catalog 017-000-121), anti–guinea pig (catalog 706-035-148) and anti–rabbit IgG-HRP (catalog 711-035-152), and anti–guinea pig FITC (catalog 706-095-148) and anti–rabbit-Cy3 (catalog 711-165-152) conjugated secondary antibodies were purchased from Jackson Immuno Research Laboratories. In situ cell death detection kit was purchased from Roche Diagnostics. Peroxo block and image FX signal enhancer was purchased from Invitrogen. All other reagents were of pure or analytical grade, and buffers were filtered through 0.45-μm Millipore filters. Every 40th pancreatic section was immunostained with guinea pig anti-insulin antibody (1:100; Invitrogen, PA1-36022) and counterstained with hematoxylin. The β cell mass for each ZDF rat was quantified using Image Pro Plus software (Media Cybernetics) by obtaining the fraction of the cross-sectional area of pancreatic tissue (exocrine and endocrine) positive for insulin staining and then multiplying this by the pancreatic weight. Apoptotic cells were detected using the TUNEL method as per manufacturer's protocol (R&D systems). For the determination of apoptosis, all β cells per pancreatic section (5 sections per animal) were analyzed to determine the total number of TUNEL-positive β cells. An average of 150 islets were counted per animal, and the percentage of TUNEL-positive cells was quantitated.

Morphometric analysis of markers of oxidative stress. To determine the presence of oxidative stress, pancreata from both control ZDF rats fed with a 17% fat diet and HFD-treated ZDF rats fed with a 48% fat diet were fixed overnight with 4% formalin. Fixed tissues were processed for paraffin embedding, and 4-μm sections were prepared and mounted on slides. Sections from both groups of animals were chosen at 25-μm intervals for immunolocalization of 4HNE, Nrf2, and HO-1, as well as insulin to identify β cells and E-cadherin to identify the pancreatic epithelium. Fifty sections per animal group were analyzed for morphometric measurements. Primary antibodies used for these experiments included anti-4HNE (Abcam, ab46545), anti-Nrf2 (Abcam, ab31163), and anti–HO-1 (Enzo Life Sciences), all used at 1:100 dilution and incubated overnight at 4°C. Following reaction with fluorophore-conjugated secondary antibodies (Jackson ImmunoResearch) slides were mounted with DAPI containing mounting medium (Vector Laboratories) and viewed at a Nikon i90 microscope for image acquisition and analysis using NIS-Elements AR 3.2 (Nikon).

ImageStream flowcytometric analysis. The ImageStreamX MarkII (Amnis, MilliporeSigma) system is an imaging flow cytometer, combining features of fluorescent microscopy and flow cytometry. Cells in suspension pass through the instrument in single file, where transmitted light, scattered light, and emitted fluorescence are collected at a rate of up to 5,000 cells/s. This is accompanied by a dedicated image analysis software (IDEAS), which allows advanced quantification of intensity, location, morphology, and population statistics within tens of thousands of cells per sample. It allows analysis of rare subpopulations in highly heterogeneous samples and gives rise to potentially novel applications that are difficult to achieve by either conventional flow cytometry or microscopy (41, 42). Cells were imaged by ImageStreamX mark II. At least 1×10^3 cells were imaged from each sample. Images were analyzed using ideas 6.2 software (Amnis, MilliporeSigma). Cells were gated first for focus using the Gradient root mean square feature then single cells using the area and aspect ratio features on the bright field image and finally intensity of DAPI positive for intact cells. To quantify the effects of the HFD vs. the control and the recovery diet, we plotted the intensity of insulin staining and the bright field area measurement, which is equivalent to cell size.

TEM. Ultrastructural analysis on pancreatic islets from control, HFD, and diet-reversed ZDF animals was performed by TEM, as previously described with minor modifications (44–46). Briefly, islets were fixed immediately after isolation at 4°C in 0.1 M sodium cacodylate buffer, pH 7.4, 2% paraformaldehyde, 2.5% glutaraldehyde (Electron Microscopy Sciences), and 3 μM $CaCl_2$. Samples were then postfixed with osmium tetraoxide (1% wt/vol in H_2O) and counterstained with uranyl acetate (2% wt/vol in H_2O).

After embedment in Durcupan resin (MilliporeSigma), ultrathin sections (70 nm) were prepared, mounted on 300 mesh gold grids, and counterstaining with uranyl acetate (1% wt/vol in H_2O) and Sato lead (1% wt/vol in H_2O). Ultrathin sections were imaged at 80 keV using an electron microscope (JEOL JEM-1230), equipped with an AMT XR80 CCD camera.

Statistics. Values are expressed as mean ± SEM. Statistical analysis was conducted using InStat Biostatistics 3.0 and Prism6, both from GraphPad Software Inc. Comparisons among the groups were done by 1- or 2-tailed Student's *t* test and 1-way ANOVA. $P < 0.05$ was considered as statistically significant.

Study approval. All procedures making use of animal subjects were reviewed and approved by the IACUC of the Pacific Northwest Diabetes Research Institute.

Author contributions

TA and JM conducted experiments of immunolocalization and morphometric analysis, collected data, and wrote first draft of the manuscript. LB, SH, and EO helped with animal studies, performed glucose and insulin tolerance tests, and collected and analyzed data. MB assisted with ImageStream flowcytometry analysis. EO provided guidance on the research strategy and helped with data analysis. VC performed studies of immunolocalization, TEM, morphometric analysis, and manuscript revision. RPR designed the experimental strategy, provided overall supervision, analyzed data, and wrote the manuscript. FU provided advice for study design and data analysis.

Acknowledgments

RPR was supported by NIH grant R01 DK38325-36, and VC was supported by NIH grant R01 DK103711 and by Program grant 4553677 from the WA State Life Sciences Discovery Fund. We also acknowledge the expert assistance of Edward Parker at the Vision Science Center, University of Washington (Seattle, Washington, USA) for ultrastructural studies by TEM. The Vision Science Center at the University of Washington (Seattle, Washington, USA) is supported by NIH NEI Center Core grant P30 EY001730.

Address correspondence to: R. Paul Robertson, Pacific Northwest Diabetes Institute, Universities of Washington and Minnesota, 720 Broadway, Seattle, WA 98122, USA. Phone: 206.799.5246; Email: rpr@pnri.org.

1. Imai Y, et al. Interaction between cytokines and inflammatory cells in islet dysfunction, insulin resistance and vascular disease. *Diabetes Obes Metab*. 2013;15 Suppl 3:117–129.
2. Santin I, Eizirik DL. Candidate genes for type 1 diabetes modulate pancreatic islet inflammation and β-cell apoptosis. *Diabetes Obes Metab*. 2013;15 Suppl 3:71–81.
3. Donath MY. Targeting inflammation in the treatment of type 2 diabetes. *Diabetes Obes Metab*. 2013;15 Suppl 3:193–196.
4. Khadija S, Veluthakal R, Sidarala V, Kowluru A. Glucotoxic and diabetic conditions induce caspase 6-mediated degradation of nuclear lamin A in human islets, rodent islets and INS-1 832/13 cells. *Apoptosis*. 2014;19(12):1691–1701.
5. Cnop M, Welsh N, Jonas JC, Jörns A, Lenzen S, Eizirik DL. Mechanisms of pancreatic beta-cell death in type 1 and type 2 diabetes: many differences, few similarities. *Diabetes*. 2005;54 Suppl 2:S97–107.
6. Rivera JF, Costes S, Gurlo T, Glabe CG, Butler PC. Autophagy defends pancreatic β cells from human islet amyloid polypeptide-induced toxicity. *J Clin Invest*. 2014;124(8):3489–3500.
7. Butler AE, Janson J, Bonner-Weir S, Ritzel R, Rizza RA, Butler PC. Beta-cell deficit and increased beta-cell apoptosis in humans with type 2 diabetes. *Diabetes*. 2003;52(1):102–110.
8. Huang CJ, et al. High expression rates of human islet amyloid polypeptide induce endoplasmic reticulum stress mediated beta-cell apoptosis, a characteristic of humans with type 2 but not type 1 diabetes. *Diabetes*. 2007;56(8):2016–2027.
9. Shalev A. Minireview: Thioredoxin-interacting protein: regulation and function in the pancreatic β-cell. *Mol Endocrinol*. 2014;28(8):1211–1220.
10. Westwell-Roper CY, Ehses JA, Verchere CB. Resident macrophages mediate islet amyloid polypeptide-induced islet IL-1β production and β-cell dysfunction. *Diabetes*. 2014;63(5):1698–1711.
11. Marselli L, et al. β-Cell inflammation in human type 2 diabetes and the role of autophagy. *Diabetes Obes Metab*. 2013;15 Suppl 3:130–136.
12. Butler PC, Meier JJ, Butler AE, Bhushan A. The replication of beta cells in normal physiology, in disease and for therapy. *Nat Clin Pract Endocrinol Metab*. 2007;3(11):758–768.
13. Mezza T, Kulkarni RN. The regulation of pre- and post-maturational plasticity of mammalian islet cell mass. *Diabetologia*. 2014;57(7):1291–1303.
14. Lipsett M, et al. The role of islet neogenesis-associated protein (INGAP) in islet neogenesis. *Cell Biochem Biophys*. 2007;48(2-3):127–137.
15. Riley KG, et al. Connective tissue growth factor modulates adult β-cell maturity and proliferation to promote β-cell regeneration in mice. *Diabetes*. 2015;64(4):1284–1298.
16. Golson ML, et al. Activation of FoxM1 Revitalizes the Replicative Potential of Aged β-Cells in Male Mice and Enhances Insulin

Secretion. *Diabetes*. 2015;64(11):3829–3838.
17. Wang Z, York NW, Nichols CG, Remedi MS. Pancreatic β cell dedifferentiation in diabetes and redifferentiation following insulin therapy. *Cell Metab*. 2014;19(5):872–882.
18. Talchai C, Xuan S, Lin HV, Sussel L, Accili D. Pancreatic β cell dedifferentiation as a mechanism of diabetic β cell failure. *Cell*. 2012;150(6):1223–1234.
19. Olson LK, Redmon JB, Towle HC, Robertson RP. Chronic exposure of HIT cells to high glucose concentrations paradoxically decreases insulin gene transcription and alters binding of insulin gene regulatory protein. *J Clin Invest*. 1993;92(1):514–519.
20. Harmon JS, Stein R, Robertson RP. Oxidative stress-mediated, post-translational loss of MafA protein as a contributing mechanism to loss of insulin gene expression in glucotoxic beta cells. *J Biol Chem*. 2005;280(12):11107–11113.
21. Kaneto H, et al. Activation of the hexosamine pathway leads to deterioration of pancreatic beta-cell function through the induction of oxidative stress. *J Biol Chem*. 2001;276(33):31099–31104.
22. Robertson RP, Zhang HJ, Pyzdrowski KL, Walseth TF. Preservation of insulin mRNA levels and insulin secretion in HIT cells by avoidance of chronic exposure to high glucose concentrations. *J Clin Invest*. 1992;90(2):320–325.
23. Gleason CE, Gonzalez M, Harmon JS, Robertson RP. Determinants of glucose toxicity and its reversibility in the pancreatic islet beta-cell line, HIT-T15. *Am J Physiol Endocrinol Metab*. 2000;279(5):E997–1002.
24. Harmon JS, Gleason CE, Tanaka Y, Poitout V, Robertson RP. Antecedent hyperglycemia, not hyperlipidemia, is associated with increased islet triacylglycerol content and decreased insulin gene mRNA level in Zucker diabetic fatty rats. *Diabetes*. 2001;50(11):2481–2486.
25. Teague J, et al. Reversibility of hyperglycaemia and islet abnormalities in the high fat-fed female ZDF rat model of type 2 diabetes. *J Pharmacol Toxicol Methods*. 2011;63(1):15–23.
26. Brereton MF, et al. Reversible changes in pancreatic islet structure and function produced by elevated blood glucose. *Nat Commun*. 2014;5:4639.
27. Harmon JS, et al. beta-Cell-specific overexpression of glutathione peroxidase preserves intranuclear MafA and reverses diabetes in db/db mice. *Endocrinology*. 2009;150(11):4855–4862.
28. Robertson RP. Chronic oxidative stress as a central mechanism for glucose toxicity in pancreatic islet beta cells in diabetes. *J Biol Chem*. 2004;279(41):42351–42354.
29. Poitout V, Robertson RP. Glucolipotoxicity: fuel excess and beta-cell dysfunction. *Endocr Rev*. 2008;29(3):351–366.
30. Tanaka Y, Gleason CE, Tran PO, Harmon JS, Robertson RP. Prevention of glucose toxicity in HIT-T15 cells and Zucker diabetic fatty rats by antioxidants. *Proc Natl Acad Sci USA*. 1999;96(19):10857–10862.
31. Tanaka Y, Tran PO, Harmon J, Robertson RP. A role for glutathione peroxidase in protecting pancreatic beta cells against oxidative stress in a model of glucose toxicity. *Proc Natl Acad Sci USA*. 2002;99(19):12363–12368.
32. Johnson DA, Johnson JA. Nrf2--a therapeutic target for the treatment of neurodegenerative diseases. *Free Radic Biol Med*. 2015;88(Pt B):253–267.
33. Guo Y, Yu S, Zhang C, Kong AN. Epigenetic regulation of Keap1-Nrf2 signaling. *Free Radic Biol Med*. 2015;88(Pt B):337–349.
34. Kanninen KM, Pomeshchik Y, Leinonen H, Malm T, Koistinaho J, Levonen AL. Applications of the Keap1-Nrf2 system for gene and cell therapy. *Free Radic Biol Med*. 2015;88(Pt B):350–361.
35. Kang JS, et al. The cytoprotective effects of 7,8-dihydroxyflavone against oxidative stress are mediated by the upregulation of Nrf2-dependent HO-1 expression through the activation of the PI3K/Akt and ERK pathways in C2C12 myoblasts. *Int J Mol Med*. 2015;36(2):501–510.
36. Tebay LE, et al. Mechanisms of activation of the transcription factor Nrf2 by redox stressors, nutrient cues, and energy status and the pathways through which it attenuates degenerative disease. *Free Radic Biol Med*. 2015;88(Pt B):108–146.
37. Yagishita Y, et al. Nrf2 protects pancreatic β-cells from oxidative and nitrosative stress in diabetic model mice. *Diabetes*. 2014;63(2):605–618.
38. Uruno A, et al. The Keap1-Nrf2 system prevents onset of diabetes mellitus. *Mol Cell Biol*. 2013;33(15):2996–3010.
39. Masuda Y, et al. The effect of Nrf2 pathway activation on human pancreatic islet cells. *PLoS ONE*. 2015;10(6):e0131012.
40. Mahadevan J, et al. Ebselen treatment prevents islet apoptosis, maintains intranuclear Pdx-1 and MafA levels, and preserves β-cell mass and function in ZDF rats. *Diabetes*. 2013;62(10):3582–3588.
41. Zuba-Surma EK, Kucia M, Abdel-Latif A, Lillard JW, Ratajczak MZ. The ImageStream System: a key step to a new era in imaging. *Folia Histochem Cytobiol*. 2007;45(4):279–290.
42. McGrath KE, Bushnell TP, Palis J. Multispectral imaging of hematopoietic cells: where flow meets morphology. *J Immunol Methods*. 2008;336(2):91–97.
43. Ahrén J, Ahrén B, Wierup N. Increased β-cell volume in mice fed a high-fat diet: a dynamic study over 12 months. *Islets*. 2010;2(6):353–356.
44. Diaferia GR, et al. β1 integrin is a crucial regulator of pancreatic β-cell expansion. *Development*. 2013;140(16):3360–3372.
45. Miller R, et al. Switching-on survival and repair response programs in islet transplants by bone marrow-derived vasculogenic cells. *Diabetes*. 2008;57(9):2402–2412.
46. Gutiérrez GD, et al. Pancreatic β cell identity requires continual repression of non-β cell programs. *J Clin Invest*. 2017;127(1):244–259.